

Less is more: Silicate on crystallization of hydroxyapatite in simulated body fluids

Ya-Nan Wang,^{a,b} Shuqin Jiang,^b Haihua Pan,^{*a} and Ruikang Tang^b

a. Qiushi Academy for Advanced Studies, Zhejiang University, Hangzhou, Zhejiang, China. 310027 E-mail: panhh@zju.edu.cn

b. Department of Chemistry, Zhejiang University, Hangzhou, Zhejiang, China. 310027 E-mail: rtang@zju.edu.cn

Table of Contents

S1 Materials and methods

S2 Measurement of the specific surface area

S3 Supplementary tables

S4 Supplementary figures

S5 Supplementary references

S1 Materials and methods

All chemicals were analytical grade and were purchased from Aladdin Reagent (Shanghai, China) unless specifically mentioned. Double distilled water was used and all stock solutions were filtered through 0.22 μm millipore films prior to use.

The SBF solutions were obtained by rapid mixing of equal volumes (5 mL) of designated calcium solutions (Ca solutions) and phosphate solutions (P solutions), and the final concentrations of each species were listed in Table S1. Ca solutions contained CaCl_2 , MgCl_2 and P solutions contained Na_2HPO_4 , Na_2SO_4 , NaCl , KCl , N-2-hydroxyethylpiperazine-N'-2-ethanesulfonic acid (HEPES, GenomBioMed Technology Inc., Hangzhou, China). Sodium metasilicate stock solutions ($\text{Na}_2\text{SiO}_3 \cdot 9\text{H}_2\text{O}$) was introduced to initial P solutions before mixing. The pH of the P solutions was pre-adjusted with $1.0 \text{ mol} \cdot \text{L}^{-1}$ NaOH or $1.0 \text{ mol} \cdot \text{L}^{-1}$ HCl to get designated SBF solutions with pH of 6.80 ± 0.04 . All experiments were conducted at temperature of 37.0 ± 0.2 °C. Each experiment has been repeated at least for four times (Figure S8).

The suspension was centrifuged at 10,000 g for 2 min (Eppendorf model 5418), and washed with double distilled water and ethanol successively, and dried in vacuum at 30 °C. After vacuum drying, the samples were analysed by FTIR, XRD, XPS, and SEM. The mineral phase and crystallinity were characterized by FITR (Shimadzu Irtfinity-1) and XRD (Rigaku D/MAX-2550pc). The morphology of the solid samples was observed by transmission electron microscope (TEM, JEOL 2100F, 200kV; Hitachi HT-7700, 100kV). For TEM/SAED/EDX examination, the samples were obtained by paddling copper grid in suspension, and washing with water and ethanol, and lamp-light dried. The hydrodynamic diameter of silicate aggregates with various concentrations (0.05-8 mM) in 5 mL P solutions were measured by dynamic light scattering (DLS) (Zetasizer Nano S, Malvern). The pH of the P solutions was pre-adjusted with $1.0 \text{ mol} \cdot \text{L}^{-1}$ HCl to get designated solutions containing silicate with pH of 6.80 ± 0.1 . Scattering data were collected for at least 50 individual measurements at a constant scattering angle and averaged for each sample. The hydrodynamic diameter of the samples was obtained using the Stokes–Einstein relationship. The Malvern Zetasizer Nano ZS instrument was also used to measure zeta potential at 25°C for silicate solutions. All DLS analyses were carried out at 25 °C. For quantitative EDX and XPS examination, a mass of dried ACP powder were pressed into a tablet by a powder tableting machine (FW-4A), and then analysed by EDX (SEM, HITACHI S4800, 5 kV, 10 μA) and XPS (ESCALAB, 250 μm), respectively.

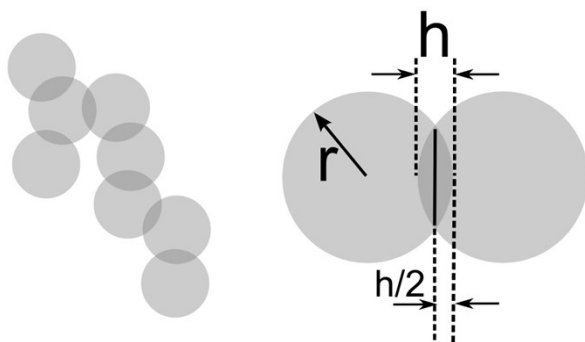
S2 Measurement of the specific surface area

TEM image directly show the state of aggregates, but care should be taken to the overlap region. The overlap in a TEM image does not represent the actual overlap in real 3D space because a TEM image is a projection of a 3D volume. So, the challenge in the analysis of a TEM image is to obtain the real overlap parameter of aggregates. Fortunately, this problem has been solved in previous work,^[S1] which has been widely applied in the study of aggregates.^[S2-S6] It was corroborated that the real overlap parameter (in 3D volume, C_{ov}) can be obtained from the projected one (in TEM image, $C_{ov,proj}$),^[S1]

$$C_{ov} = 1.1C_{ov,proj} - 0.2$$

The projected overlap parameter can be directly obtained from TEM images, where all the position and size of particles can be measured by the ImageJ software.^[S7-S8]

In the followings, we will tell how to calculate the specific surface area of aggregates from the overlap parameter and the radius of particles.



Scheme S1. The partial overlapped ACP spherules.

For partial merged ACP aggregates, it can be simplified as partial overlapped spheres (Scheme. S1). To estimation of specific area (surface area per unit volume of a material) of aggregates, one need to take into account the overlap parameter (C_{ov}) of primary particles, which is given as,

$$C_{ov} = \frac{h}{2r} \quad (S1)$$

where h is the overlap of two spheres. The total surface area (A_{ACP}) and the total volume (V_{ACP}) of aggregates can be obtained by,

$$\begin{aligned} A_{ACP} &= A_{spheres} - A_{caps} \\ &= \sum_i A_i - \sum_{i,j} A_{cap,i,j} = N([A] - N_c[A_{cap,i}]) \end{aligned} \quad (S2)$$

$$\begin{aligned} V_{ACP} &= V_{spheres} - V_{caps} \\ &= \sum_i V_i - \sum_{i,j} V_{cap,i,j} = N([V] - N_c[V_{cap,i}]) \end{aligned} \quad (S3)$$

where both the surface area and the volume of caps that embedded inside aggregates should be discounted from the each sphere of aggregates. $[X]$ is the mean value for X ; N is the total number; N_c is the coordination number of each sphere, which means on average, how many particles are overlapped with a particle. The surface area and volume of a cap with height of $h/2$ is given as,

$$A_{cap} = 2\pi r \left(\frac{h}{2}\right) = 4\pi r^2 \frac{1}{2} \left(\frac{h}{2r}\right) = [A] \frac{1}{2} C_{ov} = f[A] \quad (S4)$$

$$V_{cap} = \frac{1}{3}\pi\left(\frac{h}{2}\right)^2\left(3r - \frac{h}{2}\right) = \frac{4}{3}\pi r^3\left(\frac{3}{4}\left(\frac{h}{2r}\right)^2 - \frac{1}{4}\left(\frac{h}{2r}\right)^3\right) \quad (S5)$$

$$= [V]\left(\frac{3}{4}C_{ov}^2 - \frac{1}{4}C_{ov}^3\right) = g[V]$$

Combining Eq. S2-S5,

$$A_{ACP} = N[A](1 - fN_c) \quad f = \frac{1}{2}[C_{ov}] \quad (S6)$$

$$V_{ACP} = N[V](1 - gN_c) \quad g = \frac{3}{4}[C_{ov}]^2 - \frac{1}{4}[C_{ov}]^3 \quad (S7)$$

The specific surface area (Sa) is give as,

$$S_a = \frac{A_{ACP}}{V_{ACP}} = \frac{N[A](1 - fN_c)}{N[V](1 - gN_c)} = \frac{3(1 - fN_c)}{[r](1 - gN_c)} \quad (S8)$$

where f and g can be determined by Cov (cf. Eq. S6, S7). So, for aggregates, given the overlap parameter (Cov), the mean radius of primary particles ([r]), and the coordination number (Nc), the specific surface area can be obtained by Eq. S8. By this method, the specific surface area of ACP aggregates can be obtained by TEM images, as shown in the following figures (Fig. S10-S16).

S3 Supplementary tables

Table S1. The composition of simulated body fluid

ons	Na ⁺	K ⁺	Mg ²⁺	HPO ₄ ²⁻	Cl ⁻	SO ₄ ²⁻	Ca ²⁺	HEPES
C/mM	138.0	0.5	1.5	3.0	144.5	0.5	5.0	10.0

S4 Supplementary figures

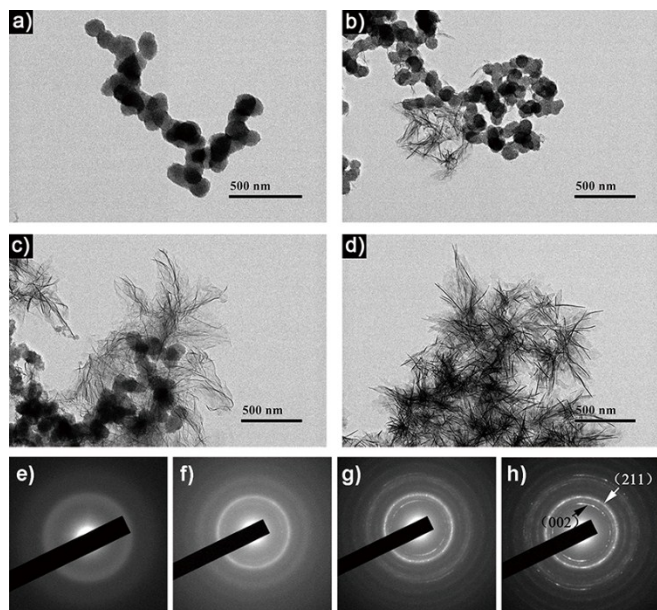


Fig. S1 HRTEM observation of precipitates and SAED patterns at designated times (as marked in Fig. 1a) of HAP formation. (a) time 1 (5 min), sphere particles of ACP; (b) time 2 (15 min), the start of HAP nucleation from ACP; (c) time 3 (20 min), coexistence of ACP and sheet-like HAP crystallites; (d) time 4 (60 min), ACP had completely transformed to HAP. Corresponding SAED patterns of these images (a-d) were given in sequence in the bottom.

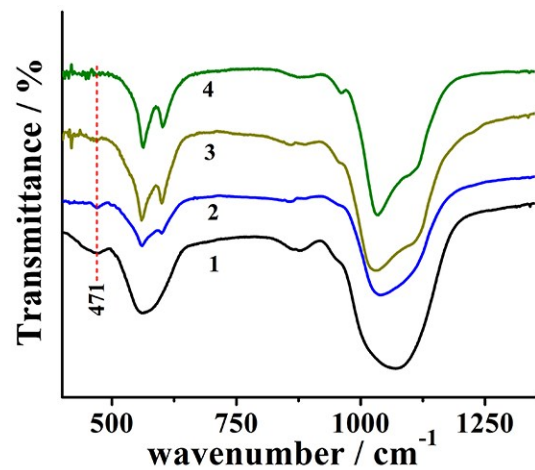


Fig. S2. FTIR spectra of minerals at different stages in the presence of 0.05 mM silicate. (1) time 1 (5 min) : amorphous calcium phosphate phase existed, the absorption at 471 cm^{-1} assigned to Si-O-Si bending mode; (2) time 2 (15 min): ACP phase transformation to HAP. The splitting of 570 and 1055 cm^{-1} absorption in FTIR indicated the crystallization of HAP; (3) time 3 (20min): the adsorption peak phosphate at 570 cm^{-1} has split into two peaks at 600 and 560 cm^{-1} , matching that of HAP; (4) time 4 (60 min): the increase of the degree of splitting corresponds with the increase of the crystallinity of HAP.

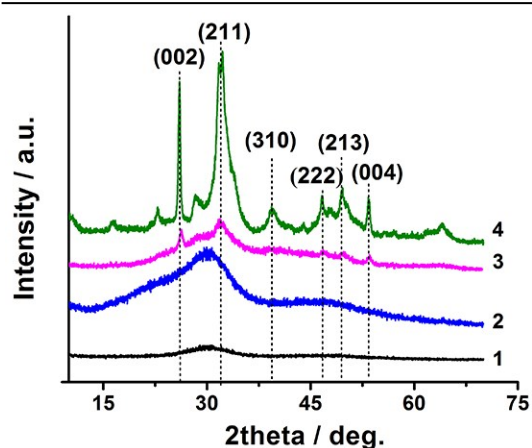


Fig. S3 Analysis of precipitates with XRD in designed time (in the presence of 0.05 mM silicate). (1) time 1 (5 min), amorphous calcium phosphate phase; (2) time 2 (15 min), the start of crystallization; (3) time 3 (20 min), the characteristic peaks of HAP appear obviously; (4) time 4 (60 min), crystallinity of HAP was increased.

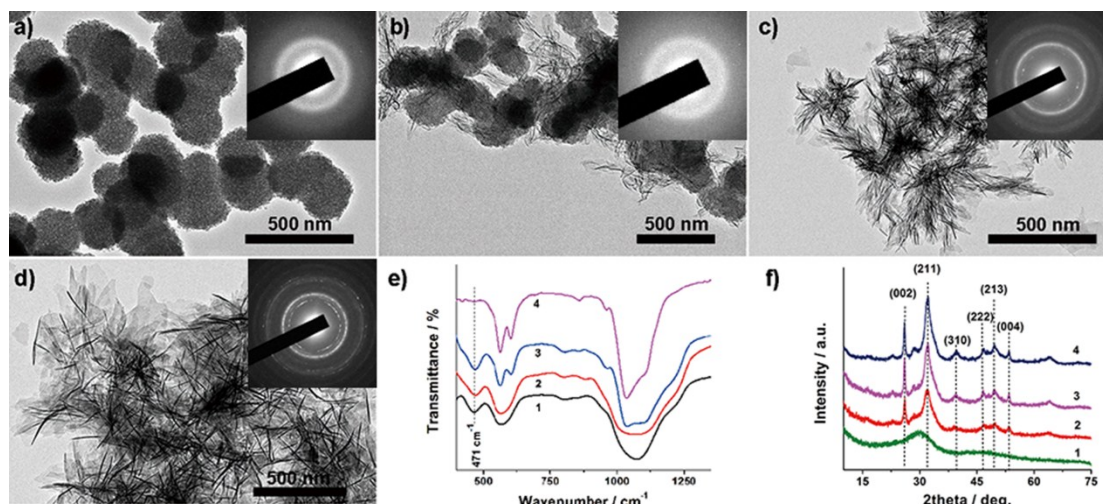


Fig. S4 HRTEM images (a-d) and the corresponding SAED patterns (inset), FTIR (e) and XRD (f) analysis of precipitates at different stages (in the presence of 8 mM silicate). (a) 10min, sphere ACP particles with rough surface; (b) 2.5h, HAP crystallites emerged out of ACP particles; (c) 3h, ACP have completely been transformed to HAP; (d) 5h, the crystallinity of HAP is increased as indicated by the SAED patterns. The ACP-mediated HAP crystallization pathway has also been confirmed by FTIR and XRD characterizations.

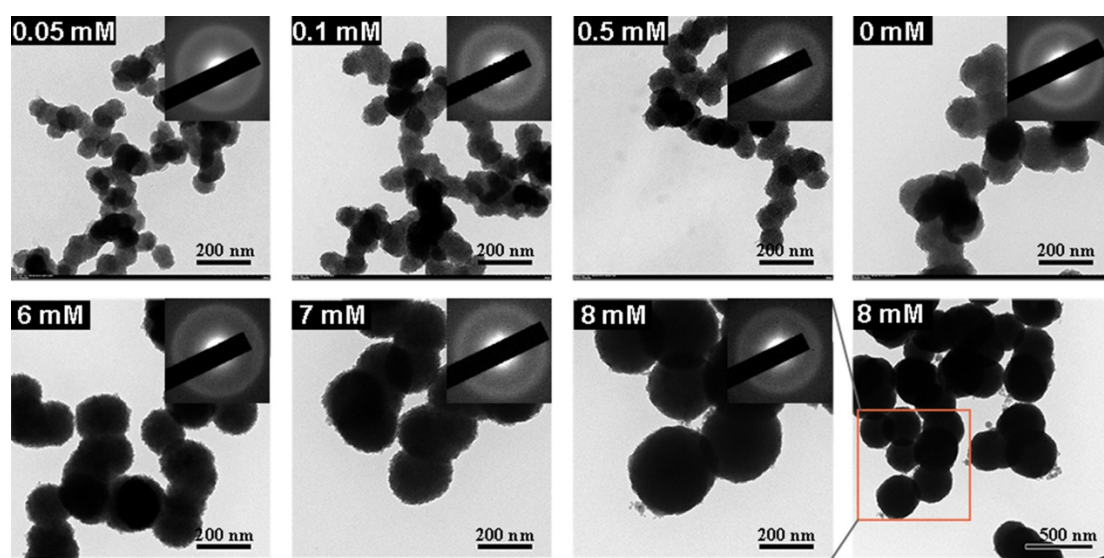


Fig. S5 TEM observation of initial ACP particles (10 min) under different concentration of silicate.

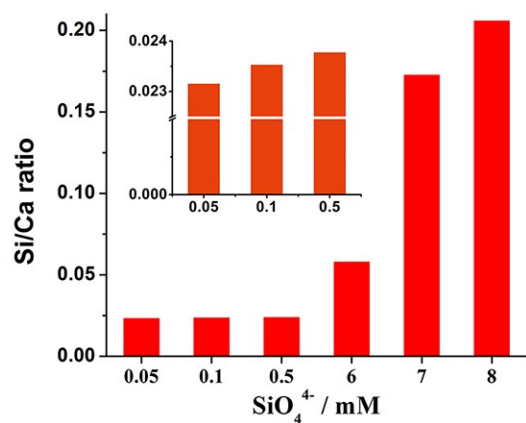


Fig. S6 The increase of Si/Ca ratio for ACPs under different concentration of silicate by the quantitative EDX analysis.

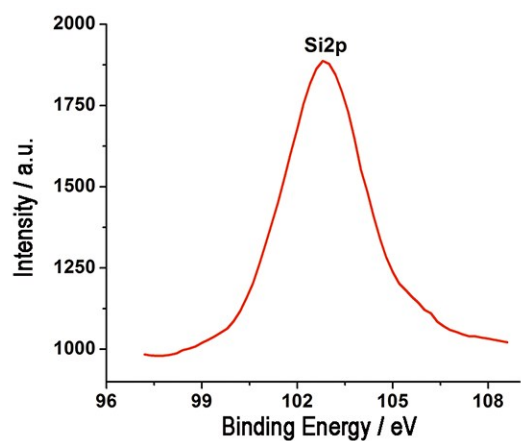


Fig. S7 Analysis of precipitates in 10 min at 8 mM silicate with XPS show the presence of silicate on ACP surface.

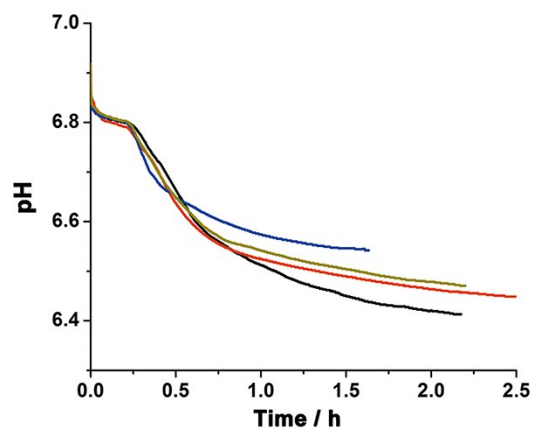


Fig. S8 The reproducibility of pH curves (0.05 mM silicate).

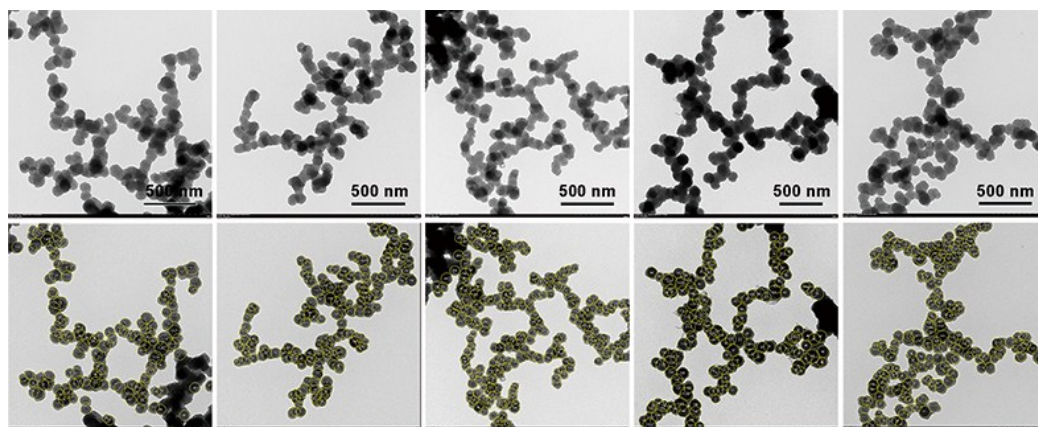


Fig. S9 The measure of primary particles for ACPs for control experiment (0.05 mM silicate) and the determination of specific surface area. (Cov: 0.56 ± 0.31 ; Nc: 2.3 ± 0.76 ; r: 56 ± 6 ; N: 931)

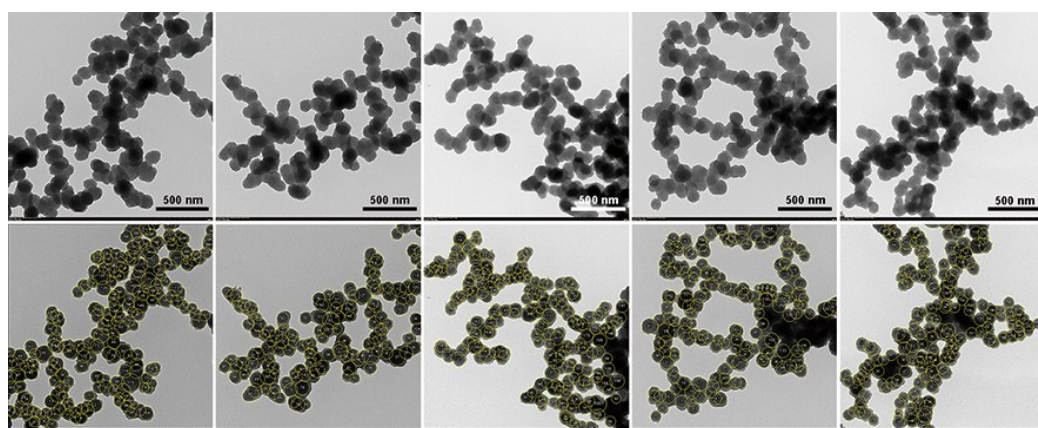


Figure S10. The mark of primary particles for ACPs (0.1 mM silicate) and the determination of specific surface area. (Cov: 0.56 ± 0.32 ; Nc: 2.32 ± 0.75 ; r: 70 ± 8 ; N: 900)

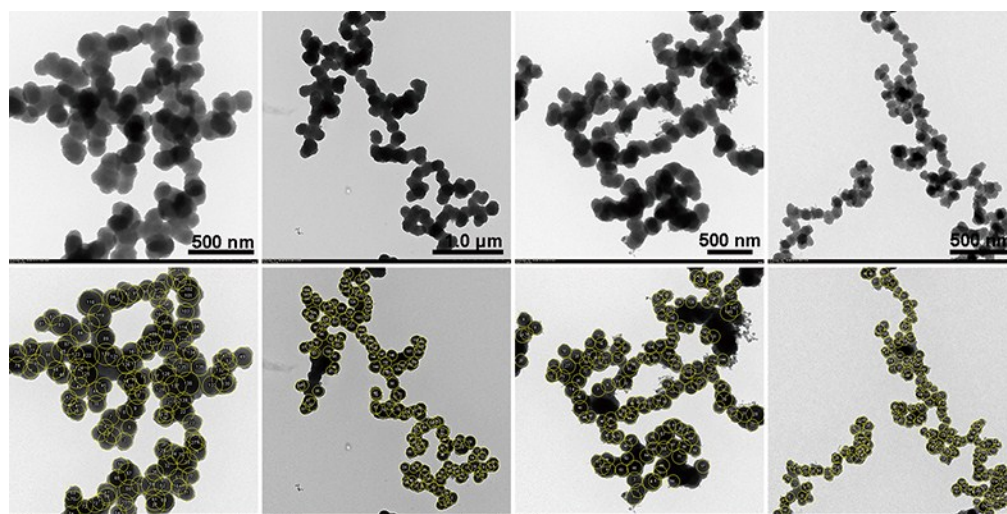


Figure S11. The mark of primary particles for ACPs (0.5 mM silicate) and the determination of specific surface area. (Cov: 0.56 ± 0.31 ; Nc: 2.3 ± 0.76 ; r: 90 ± 5 ; N: 641)

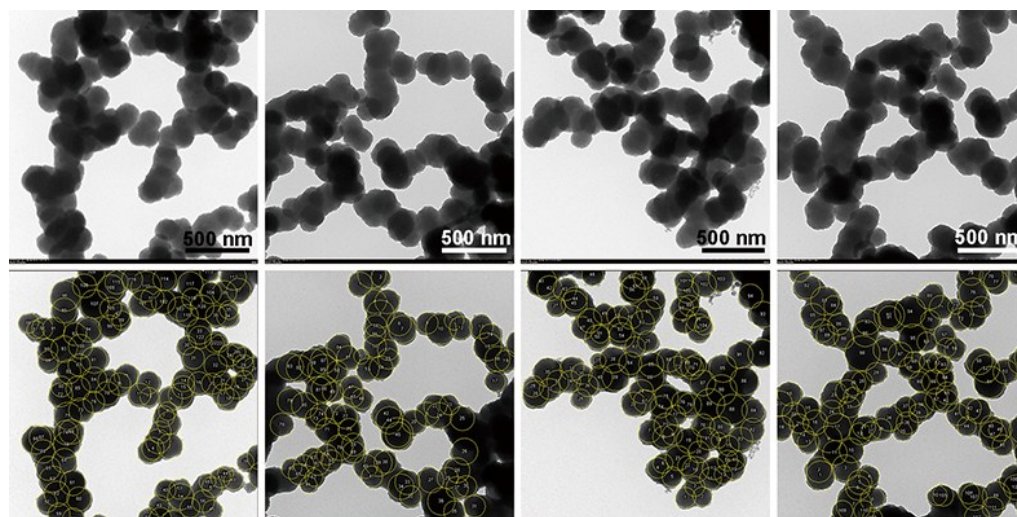


Figure S12. The mark of primary particles for ACPs (0 mM silicate / control) and the determination of specific surface area. (Cov: 0.54 ± 0.33 ; Nc: 2.43 ± 0.73 ; r: 100 ± 12 ; N: 528)

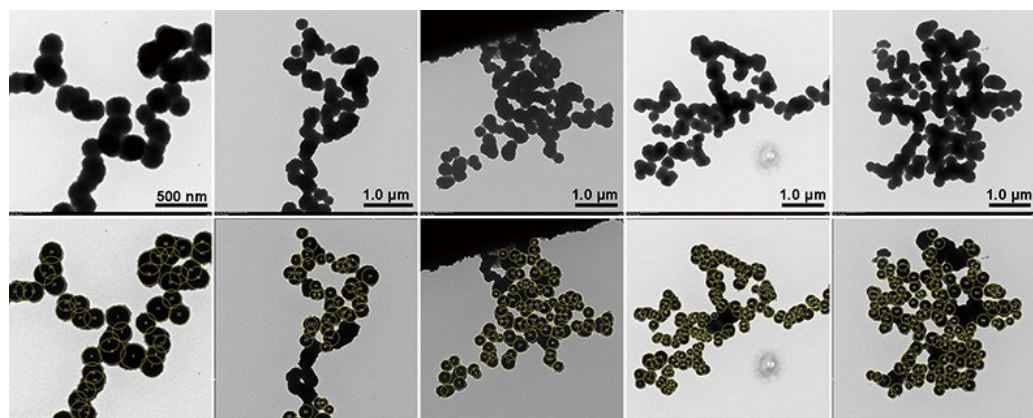


Figure S13. The mark of primary particles for ACPs (6 mM silicate) and the determination of specific surface area. (Cov: 0.55 ± 0.33 ; Nc: 2.43 ± 0.91 ; r: 130 ± 12 ; N: 558)

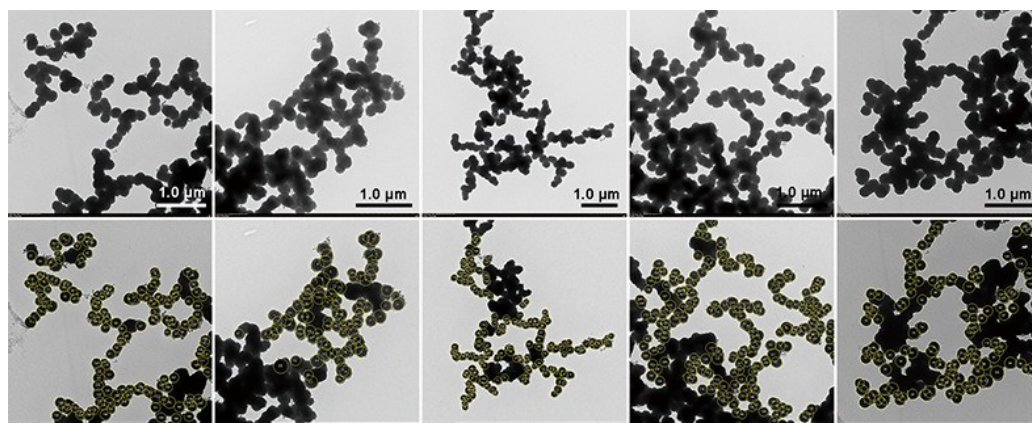


Figure S14. The mark of primary particles for ACPs (7 mM silicate) and the determination of specific surface area. (Cov: 0.57 ± 0.32 ;
 Nc: 2.44 ± 0.87 ; r: 160 ± 9 ; N: 826)

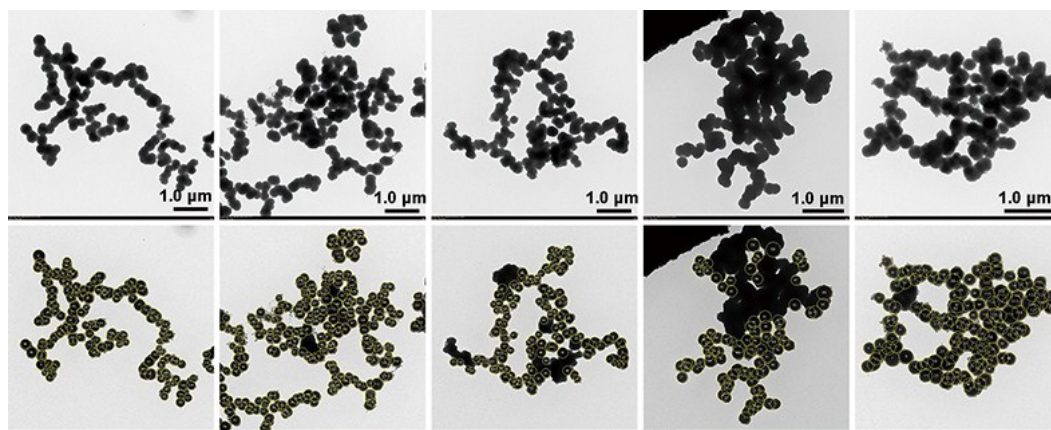
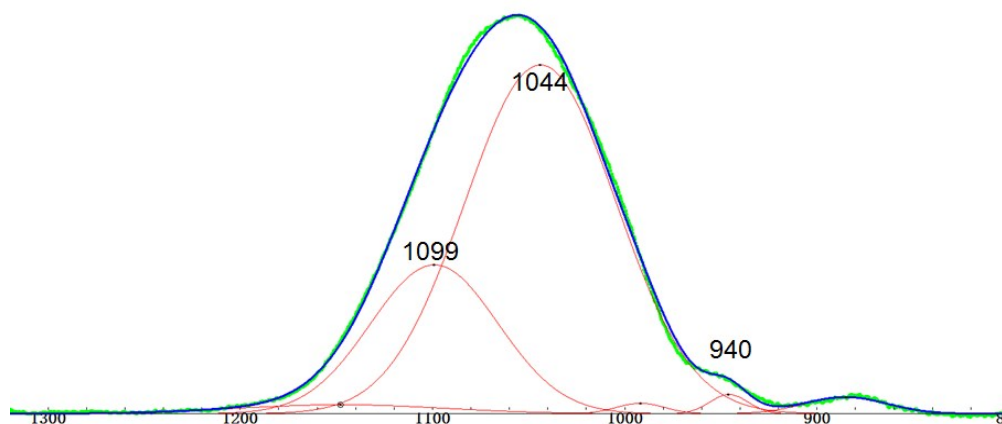
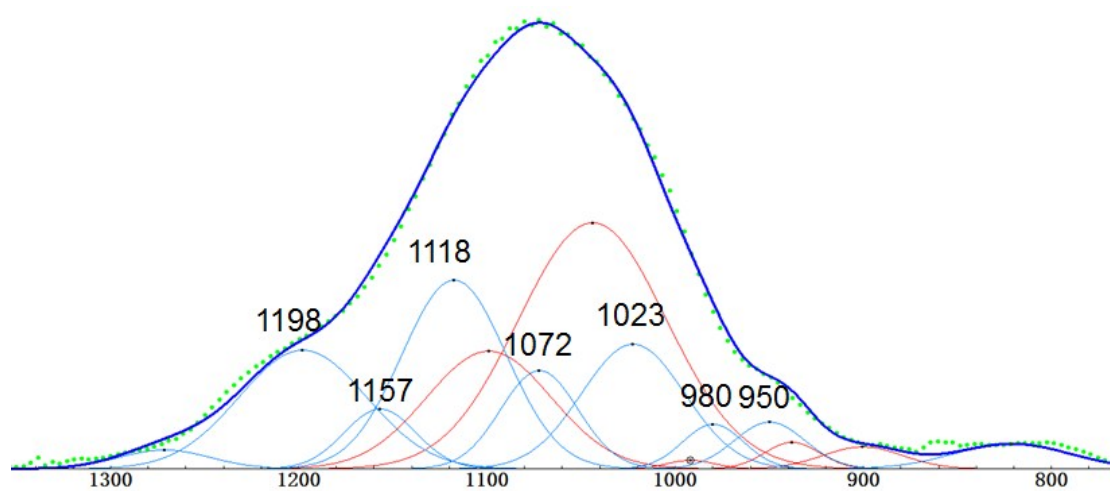


Figure S15. The mark of primary particles for ACPs (8 mM silicate) and the determination of specific surface area. (Cov: 0.59 ± 0.32 ;
 Nc: 2.46 ± 0.8 ; r: 210 ± 15 ; N: 742)

a)



b)



c)

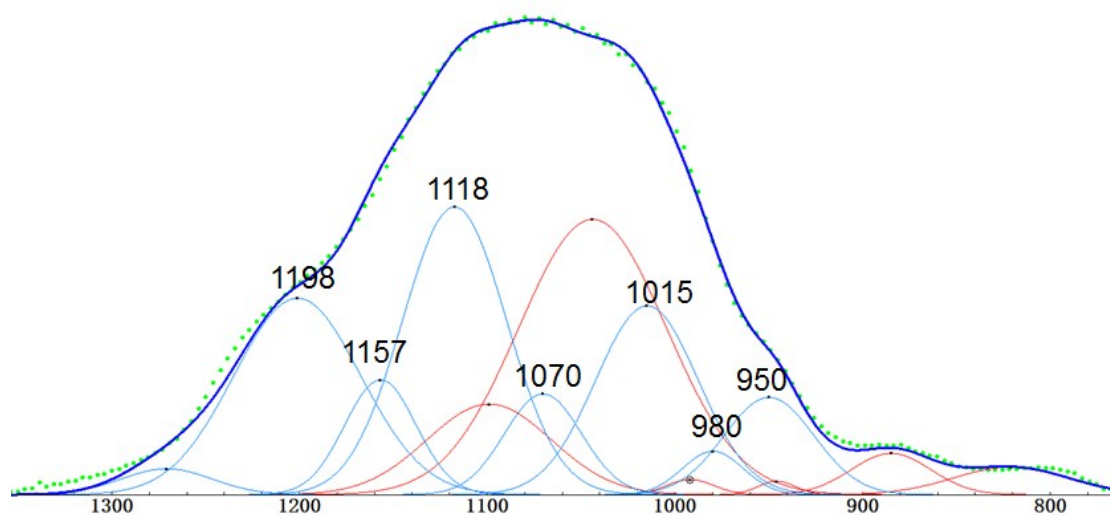


Fig. 16. The deconvolution of pure ACP (a) and ACP/silica(8mM) mineral at 10 min (b) and 2.5h (c).

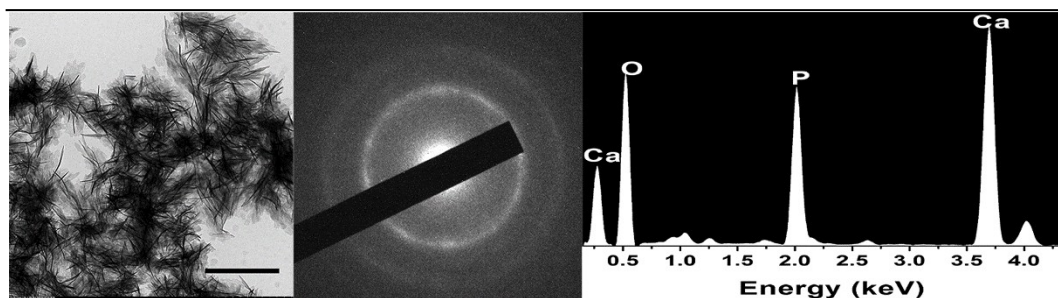


Figure S17. TEM images and the corresponding SAED patterns and EDX analysis of the final crystallized minerals (8 mM silicate).

S5 Supplementary references

- [S1] A. Brasil, T. L. Farias, M. Carvalho, *J. Aerosol Sci.* **1999**, *30*, 1379-1389.
- [S2] M. Wentzel, H. Gorzawski, K. H. Naumann, H. Saathoff, S. Weinbruch, *J. Aerosol Sci.* **2003**, *34*, 1347-1370.
- [S3] C. Xiong, S. Friedlander, *Proc. Natl. Acad. Sci.* **2001**, *98*, 11851-11856.
- [S4] W. Shin, J. Wang, M. Mertler, B. Sachweh, H. Fissan, D. H. Pui, *J. Nanopart. Res.* **2009**, *11*, 163-173.
- [S5] K. Park, D. B. Kittelson, P. H. McMurry, *Aerosol Sci. Technol.* **2004**, *38*, 881-889.
- [S6] S. China, C. Mazzoleni, K. Gorkowski, A. C. Aiken, M. K. Dubey, *Nat. Commun.* **2013**, *4*, 2122-2129.
- [S7] W. S. Rasband, <http://rsbweb.nih.gov/ij/>, **2008**.
- [S8] C. A. Schneider, W. S. Rasband, K. W. Eliceiri, *Nat. Meth.* **2012**, *9*, 671-675.